Molecular Beam Studies of the "Super" Photoacid 5-Cyano-2-naphthol in Solvent Clusters

Richard Knochenmuss,*,† Kyril M. Solntsev,‡ and Laren M. Tolbert‡

Laboratorium für Organische Chemie, Swiss Federal Institue of Technology, Universitätsstrasse 16, Zürich, Switzerland, and School of Chemistry and Biochemistry, Georgia Institute of Technology, Atlanta, Georgia 30332-0400

Received: January 4, 2001; In Final Form: April 25, 2001

Clusters of the strong excited-state acid 5-cyano-2-naphthol with water, ammonia, methanol, and Me_2SO were generated in a molecular beam and investigated by resonant two-photon ionization (R2PI) and fluorescence spectroscopies. In the free molecule and the smallest complexes these show that the S_1 state is highly analogous to that of the parent 2-naphthol. Fluorescence attributable to excited-state proton transfer (ESPT) was observed for ammonia and water clusters, but not methanol or Me_2SO. The ESPT size thresholds are, for ammonia 3 or 4; for water 8−10. The cluster ESPT characteristics of 5-cyano-2-naphthol show many similarities with those of the somewhat weaker excited-state acid 1-naphthol.

Introduction

The recently developed "super" photoacids (which are more acidic in an electronic excited state than in the ground state), such as 5-cyano-1-naphthol (5CN1NpOH) and 5-cyano-2-naphthol (5CN2NpOH), have been shown to undergo excited-state proton transfer (ESPT) to a variety of bulk solvents and solvent mixtures.[1−9] They extend the range of photoacid strength to lower pK_a* values than previously available (5CN1NpOH: −2.8[6]; 5CN2NpOH: −0.3[9]), allowing observation of a range of proton-transfer reactions that shed light on key aspects of proton solvation and transport in solution. For example, 5CN1NpOH was used to show that the intrinsic rate of proton transfer to water falls between the longitudinal and Debye relaxation times, and that the activation energy corresponds to that of water dielectric relaxation.[6]

The solvatochromism of 5CN2NpOH and the parent 2-naphthol (2NpOH) has been discussed in terms of the Kamlet−Taft solvation parameters.[2,9,10] The hydrogen bond (HB) donating or accepting properties of the solvent were thereby correlated with the shifts in band positions of the unreacted molecule and the post-ESPT anion. Anion solvation and the proton free energy of transfer were found to be the major determinants of the pK_a* values in different solvents. This in turn determines the time scale of ESPT in solution according to the Agmon-Levine relationship between reaction free energy and rate.[11,12] The ESPT reaction in protic solvents was proposed to proceed in the S_1 state by cleavage of the proton-donating HB from the solvent to the hydroxyl oxygen of the naphthol, with concurrent strengthening of the HB in which the solvent accepts the proton from the naphthol hydroxyl.

Time resolved 5CN2NpOH solution fluorescence was found to be well fit by a Debye−Smoluchowski equation for reversible geminate recombination, taking into account different lifetimes and quenching rates for the neutral and anion.[4,9,13] The ESPT forward dissociation time constant was found to be 20 ps in water and 4−8 ns in other protic and nonprotic solvents. Quenching was strong in all cases, and the quantum yields were low, especially in water.

The closely related compounds 1- and 2-naphthol are important prototype ESPT-active substances in water solution.[5−7,10,14−25] A deeper understanding of these reactions was achieved by molecular beam/laser spectroscopy studies of the free molecules and their clusters with various solvents. 1-Naphthol (1NpOH) has been especially well studied, particularly in ammonia[21,26−35] and water[18−22,36,37] clusters. 2-Naphthol (2NpOH) was found to undergo ESPT in ammonia,[38] but not in water clusters.[20] For both 1- and 2-naphthol the cluster size threshold for EPST was found to be 4 ammonia molecules.[26,28,34,35,38] This is the same threshold found for phenol-ammonia clusters,[39,40] but it should be noted that phenol clusters display much more complex behavior than naphthols, including excited-state hydrogen atom transfer reactions,[41−43] and more extensive fragmentation.[41−45]

In clusters of 1NpOH with ammonia, the base is believed to cause preexcitation L_b/L_a state mixing, and the reaction can be characterized as evolution on the S_1 excited-state hypersurfaces.[30] This reaction type has been termed adiabatic.[30] The corresponding 2NpOH reaction has not yet been investigated in equal detail, but shows strong similarities in such aspects as size threshold for ESPT and extent of ESPT at the threshold.[38]

Clustered with the weak base water, the ESPT reaction of 1NpOH was found to be an activated process involving multiple time scales which are believed to be determined by solvent reorganization.[18−20,30] The cluster size threshold is rather large (25−30),[18] and this reorganization was found to take place around the entire molecule, as an extended dipole develops.[46] This reaction type has been termed nonadiabatic, and is dependent on the dynamic solvent response to the change in electronic state.[30] Since the initially excited state has long been known to be only weakly affected by the solvent, a trigger for ESPT is needed. This was proposed to be vibronic coupling of the first 2 excited states, which mixes polar S_2 (initially L_a) character into the lower, less polar, S_1 (initially L_b) state.[46,47] The feedback between solvent response and electronic state mixing leads to S_1/S_2 state inversion, which is followed or accompanied by proton transfer to the lower-lying anion

* Author for correspondence. E- mail: knochenmuss@org.chem.ethz.ch. Phone: ++41 1632 3875. Fax: ++41 1632 1292.
† Laboratorium für Organische Chemie.
‡ School of Chemistry and Biochemistry.

10.1021/jp010011u CCC: $20.00 © 2001 American Chemical Society
Published on Web 06/12/2001

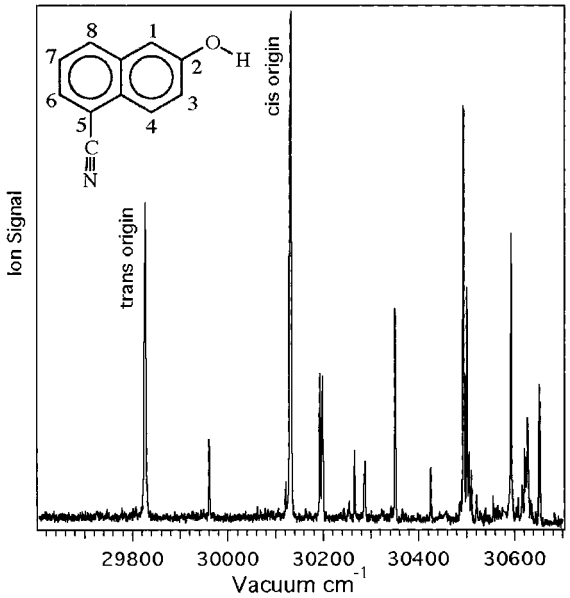

Figure 1. Resonant two-photon ionization spectrum of 5-cyano-2-naphthol in the electronic origin region, detected at $m/z = 169$ Da. Two rotational isomers are detected, as for the parent 2-naphthol. The ionization laser was set at 39600 cm^{-1}. The inset shows the cis rotamer of 5-cyano-2-naphthol with the conventional numbering system.

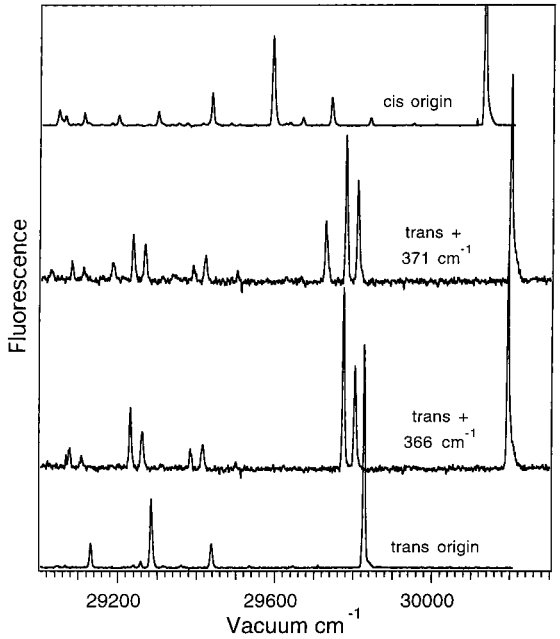

Figure 2. Fluorescence spectra of 5-cyano-2-naphthol, either at the electronic origin of the two rotamers or following excitation of single vibrational levels in the trans rotamer. The largest, rightmost peak in each spectrum is predominantly scattered laser excitation light.

state.[30,46] Magnes et al. have shown that the inversion can be induced without ESPT,[48] so it presumably precedes the actual transfer event when the reaction occurs.

For 2NpOH in water solution, the ESPT reaction was found to be strongly activated,[25] and at lower temperatures (above 0 °C) becomes too slow to compete with decay of the initially prepared excited state. As expected from this fact, no ESPT was observed in cold water clusters.[20] In contrast to 1NpOH, there is at present no evidence that the S_1 (L_b) and S_2 (L_a) states are inverted prior to proton transfer in water solution.[48] Despite the lack of ESPT, 2NpOH−water clusters are proving to be a very profitable object of study, and a great deal has been learned about hydrogen bonding from them.[49,50]

The present work is an initial effort to use clusters as a complement to solution studies to develop a more detailed mechanistic understanding of ESPT reactions of stronger photoacids, as was possible for 1-naphthol. It also provides a test of some concepts developed earlier by comparing clusters of the same proton acceptors with different, stronger acids. Among the interesting questions are the clusters size thresholds for ESPT, the static and dynamic solvation contributions to ESPT, the rates of ESPT and quenching in slowly relaxing cold clusters, and the role of vibronic coupling as a trigger for the reaction. In addition, the spectroscopy of cyano naphthols is of intrinsic interest, especially for improving the understanding of substituent effects on excited states.

Experimental Section

5-Cyano-2-naphthol was synthesized and purified as described in ref 1. The molecular beam spectroscopy methods were similar to those reported in earlier studies.[26,28] The naphthol was entrained in a stream of carrier gas at a total pressure of 1−3 bar. Neon was used as carrier, and the solvent species were either added in gaseous form (0.5% NH_3), or introduced by bubbling the gas through the liquid solvent at room temperature just before it passed into the nozzle assembly. The naphthol vapor pressure was regulated by heating the nozzle, typically temperatures of 140−160 °C were used (melting point 179−180 °C[1]). This mixture was expanded through a pulsed valve into a vacuum. After skimming, the cooled molecules were excited with unfocused nanosecond pulses from frequency doubled pulsed, Nd:YAG-pumped dye lasers. The resulting ions were mass analyzed in a 1 m linear time-of-flight mass spectrometer. The laser was scanned while observing the relevant mass peak with a transient digitizer.

TABLE 1: S_1 Electronic Origin Positions and Some Vibrational Frequencies Observed in the R2PI Spectra of the Two Rotamers of 2-Naphthol and 5-Cyano-2-naphthol, in (cm^{-1})[a]

trans 2N/ 30586 origin	trans 5C2N/ 29826 origin	cis 2N/ 30903 origin	cis 5C2N/ 30133 origin
	135		133
203		203	208
238	234	237	234
273		271	
288	294	287	293
385	366	384	362
397	371	395	368
397		395	
408		409	
451	461	451	462
490		491	489
498		496	495
	524		520

[a] The 2-naphthol frequencies and trans/cis assignments are from ref 53.

Two-color two-photon ionization experiments were performed by attenuating the pump and ionization lasers until 1-color signals were absent or very nearly so. Residual one-color signal was measured separately and subtracted. Fluorescence spectra were measured with an f/4 optical system, including a SPEX 500 M 0.5 m grating monochromator (150 or 2400 lines/mm gratings) and detected with a CCD array (Princeton Instruments, 2500 × 600 pixels).

Wavelength-selective fluorescence decay curves were measured on the same monochromator using a Hamamatsu R3896 photomultiplier and a LeCroy LC574AM digital oscilloscope.

TABLE 2: Calculated vs Observed S_0 Vibrations of 5-Cyano-2-naphthol, in cm^{-1} [a]

cis rotamer			trans rotamer		
6-31G (d,p)*0.9	symmetry/description	experiment, cm^{-1}	6-31G (d,p)*0.9	symmetry/description	experiment, cm^{-1}
	origin	30 133		origin	29 826
92.7	OH + CN op wag		91.8	CN op wag	
128.7	CN ip wag	118	128.7	CN ip wag	125
131.4	a″		131.4	a″	
200.7	OH torsion	182	199.8	a″	181
243	a′		290.7	OH ip wag	292
290.7	a″		294.3	a″	
296.1	a′	293	330.3	OH torsion	
385.2	a′		386.1	a′	
390.6	a″	390	387.9	a″	390
429.3	a′	425	430.2	a′	423
459	a″		457.2	a″	
461.7	a′	467(461)	459	a′	464(460)
514.8	a″	511	517.5	a″	
534.6	a′	542(526)	533.7	a′	541(525)
593.1	a′	589(587)	594	CN ip bend	
617.4	CN op bend		617.4	CN op bend	
640.8	a″		641.7	a″	
682.2	a′	697	681.3	a′	695
700.2	a′		702	a′	
747.9	a″	761(772)	749.7	a″	774
804.6	a″	781	800.1	a″	
817.2	a′		815.4	a′	
831.6	a″	837	846.9	a″	
880.2	a″		856.8	a″	
931.5	a′	935	933.3	a′	932
943.2	a″		941.4	a″	
985.5	a″		990	a′	
990.9	a′		999.9	a″	
1008.9	a′		1007.1	a″	
1031.4	a′	1023	1036.8	a′	1020
1094.4	a′	1088	1100.7	a′	
1149.3	a′		1138.5	a′	
1156.5	a′		1158.3	a′	
1183.5	OH ip bend		1177.2	OH ip bend	
1198.8	a′		1205.1	a′	
1240.2	a′	1242	1244.7	a′	1241
1264.5	a′	1254	1263.6	a′	
1332	a′		1323	a′	
1341	a′		1350.9	a′	1349
1381.5	a′	1381	1377		1375

[a] The values in paranthesis are for 2-naphthol, from ref 52. The basis used was 6-31G(d,p).

The analog bandwidth was 1 GHz, and the waveform was repetitively sampled at 10 GHz (2GHz single shot sample rate). The acquisition was triggered with a fast photodiode from scattered laser light. The time = 0 position and the instrument response function were obtained by observing Brillouin-scattered laser light with the vacuum chamber filled with nitrogen.

Ab initio RHF and complete active space-MCSCF quantum chemical calculations were performed with the GAMESS package (Macintosh version).[51]

Results and Discussion

(1) Free 5-Cyano-2-naphthol. The resonant two-photon ionization (R2PI) and fluorescence spectra of 5-cyano-2-naphthol (5CN2NpOH) are shown in Figures 1 and 2, and are very similar to the noncyano analogues; compare Tables 1 and 2. As observed for 2-naphthol (2NpOH), there are two rotamers in the molecular beam, differing by the orientation of the hydroxyl with respect to the ring.[38,52,53] These are assigned here by analogy to the rotationally resolved 2NpOH results of Johnson et al.[53]

The origin red shifts vs 2NpOH are 761 and 772 cm^{-1} for the cis and trans 5CN2NpOH rotamers, respectively. The difference in rotamer origin positions is nearly the same: 2NpOH = 318, 5CN2NpOH = 307 cm^{-1}. The cyano derivatives exhibit more extensive vibrational structure in fluorescence. The increased density of active modes in 5CN2NpOH is presumably associated with the transfer of charge to or from the CN group upon excitation, which couples the electronic transition to vibrations involving the CN. Nevertheless, the vibronic structure in both absorption and emission indicates that the S_1 of 5CN2NpOH is very similar to that of the 2NpOH parent, and thus has more short-axis character than the S_1 of 1-naphthol.[53] This also means that the proton transfer reactions of the two species can be straightforwardly compared, they do not begin from fundamentally different excited states. The same conclusion was reached from steady-state solution measurements.[9,10,48]

The origin-excited fluorescence spectra of the two 5CN2NpOH rotamers are, as expected, very similar, but the S_0 vibrational frequencies observed are mostly quite different from those in the S_1 states. This is one possible indication of a rotation of normal modes between S_0 and S_1, which can be induced by vibronic coupling between S_1 and S_2. This effect is among the most important aspects of the 1NpOH ESPT reaction in water. Vibronic coupling appears to trigger the reaction by adding more polar L_a character to the low polarity L_b state.[30,46]

The role of vibronic coupling in 2-naphthols has not yet been extensively studied, but indications of it are found in Figure 2. Excitation of the close-lying bands at 366 and 371 cm^{-1} above

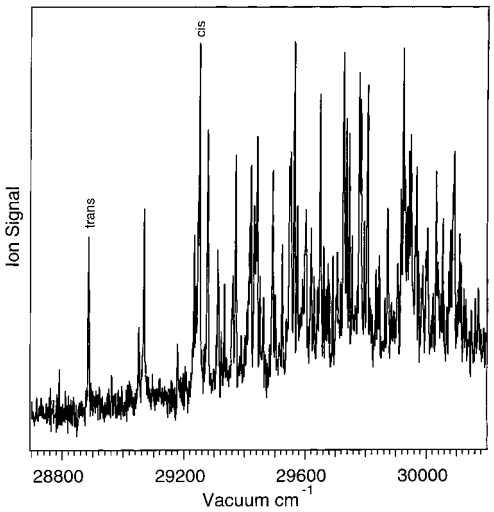

Figure 3. Resonant two-photon ionization spectrum of the 5-cyano-2-naphthol(NH3) complex in the electronic origin region, detected at $m/z = 169 + 17 = 186$ Da. Two rotational isomers are detected, as for the free molecule. The vibrational structure is very extensive. The ionization laser was set at 39600 cm^{-1}.

the trans origin gives rise to the middle two spectra. As is typical for vibronic coupling, there are multiple strong bands in the "$\Delta v = 0$" region (near 29800 cm^{-1}), instead of a single band. From Figure 2 the two ground state vibrations that are strongly mixed in the S_1 have S_0 energies of 390 and 420 cm^{-1}. These are near the energies where vibronic coupling was found for 1-naphthol. The 420 cm^{-1} mode is not observed in the origin fluorescence. "Missing" bands are a type of absorption/emission asymmetry that is frequently characteristic of normal mode rotations.

(2) 5-Cyano-2-naphthol Ammonia Clusters. The parent compound, 2-naphthol, exhibits well resolved, highly structured $S_1 \leftarrow S_0$ R2PI spectra for $2NpOH(NH_3)_n$ clusters of up to $n = 3$.[38] At and above $n = 4$, vibrational structure is lost. In contrast, only the $5CN2NpOH(NH_3)_1$ cluster is found to have a resolved absorption spectrum, as shown in Figure 3. Already at this cluster size, the spectral congestion is heavy, far more so than for $2NpOH(NH_3)_1$ and rather similar to $2NpOH(NH_3)_3$. The presence of the cyano group thus has a large effect on the spectrum, which is expected to occur via the increased charge transfer from the hydroxyl group in the S_1, pulling the ammonia toward the naphthol[54] and thereby enhancing coupling of the electronic transition to the intermolecular modes. The observation of the 27, 59, and 170 cm^{-1} bands are, by analogy with $2NpOH(NH_3)$, consistent with the ammonia bound to the hydroxyl group. Also as for 2NpOH, the trans rotamer exhibits far less vibrational structure than the cis rotamer.

2-Naphthol undergoes ESPT in ammonia clusters with the same threshold size as for 1-naphthol, $n = 4$,[38] despite its higher pK_a^* in water (2.8 vs 0.4). This was found to be consistent with a thermodynamic model for the effect of cluster size on the reaction, via the solvent cluster proton affinity.[26] The change in 1NpOH vs 2NpOH reaction enthalpy due to differences in pK_a^* (about 3 kcal/mol) is smaller than the increment in solvent cluster proton affinity between $(NH_3)_4$ and $(NH_3)_5$ (6 kcal/mol), and thus did not change the ESPT threshold.

The pK_a^* of 5CN2NpOH in water is less than that of 1NpOH, -0.3,[9] but not dramatically so. The increment in reaction enthalpy compared to 1NpOH is estimated to be about -5 kcal/mol, slightly smaller than the PA differences of $(NH_3)_3$ and $(NH_3)_4$ (8 kcal/mol). The thermodynamic model predicts an

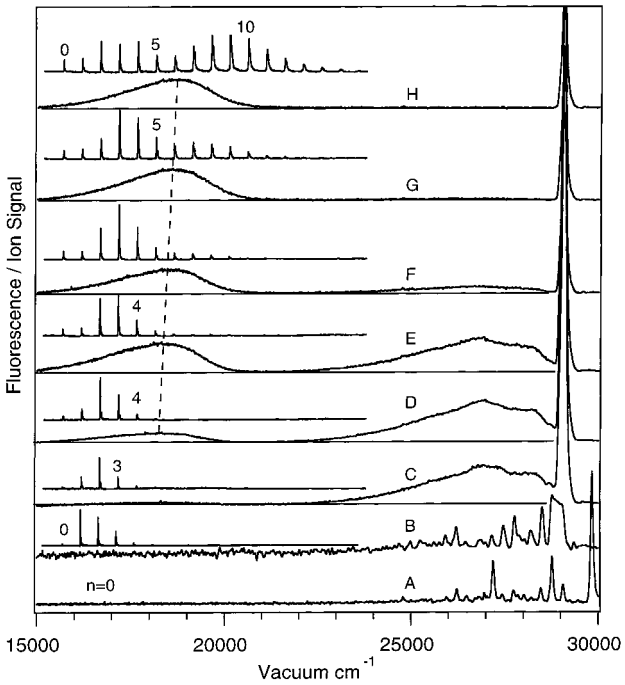

Figure 4. Fluorescence spectra of some 5-cyano-2-naphthol$(NH_3)_n$ cluster distributions. The mass spectra corresponding to the fluorescence spectra are inset on the left. Red-shifted ESPT emission appears for $n \geq 3$ or 4. Excitation was at 29100 cm^{-1} for spectra C−H, and ionization was at 36350 cm^{-1}. The free molecule was excited at the trans rotamer origin, as was the $n = 1$ cluster. The dashed line indicates the blue shift of the ESPT emission with increasing cluster size. The largest, rightmost peak in each spectrum is predominantly scattered laser excitation light. See text for further discussion.

ESPT threshold of $n = 4$ or possibly $n = 3$, for 5CN2NpOH ammonia clusters.

Figure 4 shows the fluorescence spectra obtained from the associated $5CN2NpOH(NH_3)_n$ cluster distributions. For the smallest clusters $n < 4$ (spectra B and C), the emission begins at the excitation wavelength and is about as broad as that of the free molecule (spectrum A). Consistent with the R2PI spectra, only the $n = 1$ cluster shows resolved vibrational structure; clusters with 2 or 3 ammonia molecules yield only broad vibrational envelopes, compare spectra B and C.

In spectrum D a broad new emission band is clearly apparent. It is very strongly red shifted, and centered at about 18500 cm^{-1}. This corresponds well to the deprotonated 5CN2NpOH anion emission observed in, for example, water or Me_2SO solution.[1,9] The equivalent ammonia cluster anion emission of 2NpOH lies higher, at about 22000 cm^{-1}.[38]

From spectra C and D, the ESPT band is qualitatively seen to be correlated with the appearance of $n = 3-4$, as expected. An attempt was made to quantitatively determine the ESPT threshold by comparing the anion/molecular fluorescence intensity ratios with the mass spectra. Both values fit the combined data of spectra C and D equally well, the threshold could not be determined precisely. The ESPT size threshold is thus either the same as for 1NpOH and 2NpOH, or one unit smaller.

As the cluster distribution is shifted to larger sizes in spectra E through H, the ESPT anion emission becomes dominant, and the molecular emission almost vanishes. This seems initially inconsistent with the associated mass spectra, but is not. As was studied in detail for $1NpOH(NH_3)_n$ clusters,[55] the larger clusters have lower ionization potentials, and the two-color excitation scheme used leaves them with substantial internal

energy in the ion state. They then fragment into the lower mass channels, giving the impression that many more small clusters were present than was actually the case. In spectra G and H, essentially all the signal in clusters $n < 6$ is due to such fragments. This effect can be reduced or eliminated by choice of a longer ionization wavelength, but this also leads to reduced signal of the smaller nonfragmenting clusters which have higher ionization potentials. The ionization wavelength was selected to ionize all clusters present, at the cost of some fragmentation.

The complete lack of molecular emission in spectra G and H is very probably a consequence of ground state proton transfer in larger clusters. The threshold for this is expected to be only slightly above that for excited state proton transfer. This has been experimentally observed for 1NpOH[55] and theoretically discussed.[56]

The anion band shifts slightly to the blue with increasing cluster size, as indicated by the dashed line in Figure 4. A similar effect is observed for $2NpOH(NH_3)_n$ clusters,[38] it was proposed that the emission was a superposition of contact ion pair and solvent-separated ion pair bands. The latter becomes more likely in larger clusters where the proton can diffuse away. The solvent-separated anion was proposed to emit at higher energy.

This explanation seems unlikely in $5CN2NpOH(NH_3)_n$ clusters because the blue shift occurs over a small size range, where the diffusion range of the proton is very limited. Another possible explanation is the stronger cooling needed in the supersonic expansion to obtain the larger clusters. In the coldest clusters the extent of solvent relaxation around the anion could be decreased, as is observed in a much more dramatic way for $1NpOH(H_2O)_n$ clusters.[20]

The time dependence of the ESPT reaction can be a very important indication of the nature of the reaction, as found for 1NpOH in water and ammonia clusters.[19,20,30,35] The fluorescence decay curves of the molecular and anion emissions in Figure 4 were therefore also recorded. As is often the case, quenching processes are slower in the molecular beam than in solution (5CN2NpOH lifetime = 5−6 ns in bulk water[4,9]), indicating that they are vibrationally activated in nature. The molecular emission in the distribution of spectrum E in Figure 4 was found to have lifetime of 23 ± 2 ns at 27800 cm^{-1}. The anion fluorescence at 17100 cm^{-1} has a much longer lifetime of 50 ± 2 ns.

An interesting aspect of the fluorescence decay curves is that anion emission appears 2−3 ns later than that of the unreacted clusters. Either some clusters undergo an unexpectedly slow ESPT reaction, and/or there is extensive post-ESPT relaxation and dynamic Stokes shift. If ESPT is in the nanosecond range, it will be a significant difference compared to $1NpOH(NH_3)_4$ clusters, where ESPT occurs in tens of picoseconds.[30,35] It will also mean that the reaction is nonadiabatic, and dependent on slow solvent relaxation in the excited state. This is not expected for a photoacid that is stronger than 1NpOH and needs further study.

(3) 5-Cyano-2-naphthol Water Clusters. In bulk water, the 2NpOH ESPT reaction is endoergic and therefore inhibited at reduced temperatures.[25] Consistent with this, no ESPT was observed in cold water clusters.[20] In contrast, the 5CN2NpOH reaction with water is exoergic and could be expected to be efficient in clusters. By comparison with the weaker photoacid 1NpOH, the size threshold for $5CN2NpOH(H_2O)_n$ ESPT might also be expected to be smaller, less than 25.

Figure 5 shows the fluorescence spectra of some $5CN2NpOH(H_2O)_n$ cluster distributions. As for ammonia clusters, vibrational structure is lost at rather small sizes, but the emission remains

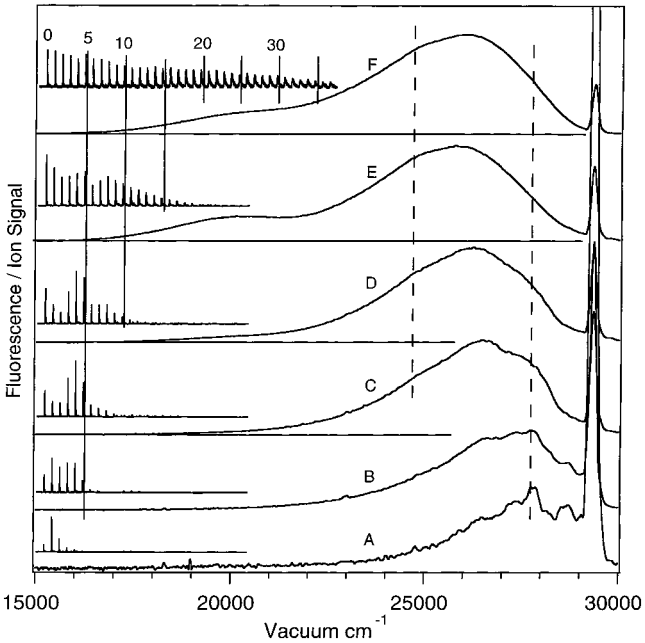

Figure 5. Fluorescence spectra of some 5-cyano-2-naphthol$(H_2O)_n$ cluster distributions. The mass spectra corresponding to the fluorescence spectra are inset on the left, and cluster size increments of 5 are indicated with vertical lines. The red-shifted ESPT emission appears for $n \geq 8-10$. Excitation was at 29100 cm^{-1}, and ionization was at 36350 cm^{-1}. The dashed lines help to compare the position and shape of the molecular emission. The largest, rightmost peak in each spectrum is predominantly scattered laser excitation light. See text for further discussion.

molecular in nature up to spectrum C. For larger distributions two changes occur. First, and most obvious, a broad new band at large red-shift develops, centered at about 20000 cm^{-1}. This is interpreted as ESPT anion emission. Second, the molecular emission region shifts generally to the red and develops a bulge on the red side of the band. This can be seen more easily with the aid of the dashed lines in the figure.

The ESPT emission is at distinctly higher energy than for ammonia clusters, and is also slightly higher than the corresponding band in liquid bulk water, at about 19500 cm^{-1}. It first appears in spectrum D as clusters of $n = 8-10$ become noticeable. In spectra E and F, where $n > 10$ are abundant, it is strong. The threshold size for ESPT is therefore near 10, less than half the size needed for $1NpOH(H_2O)_n$.

The ESPT band is clear in spectra D−F, but does not become dominant, even for the largest clusters achieved. This is in strong contrast to water solution where the anion emission is very strong. It is even weaker than in $1NpOH(H_2O)_n$ clusters, where it is at least as strong as the molecular emission. This seems a puzzling contrast to expectations from the pK_a^* values and the lower size threshold. One possible explanation is suggested by a comparison of spectra E and F. Although there are larger clusters contributing to spectrum F, the relative strength of the ESPT band is less than in spectrum E. The difference between the experimental conditions for the two spectra was a doubling of the carrier gas pressure to generate the distribution of spectrum F. The cooling in the expansion was therefore substantially greater. This led to larger, yet less reactive clusters. A very similar effect was observed for $1NpOH(H_2O)_n$ clusters, where it is found that the reaction extent and rate is very sensitive to cluster internal energy.[20] This is one significant piece of evidence leading to the nonadiabatic model in which dynamic water relaxation after photoexcitation is a key aspect of the ESPT process.[30,46]

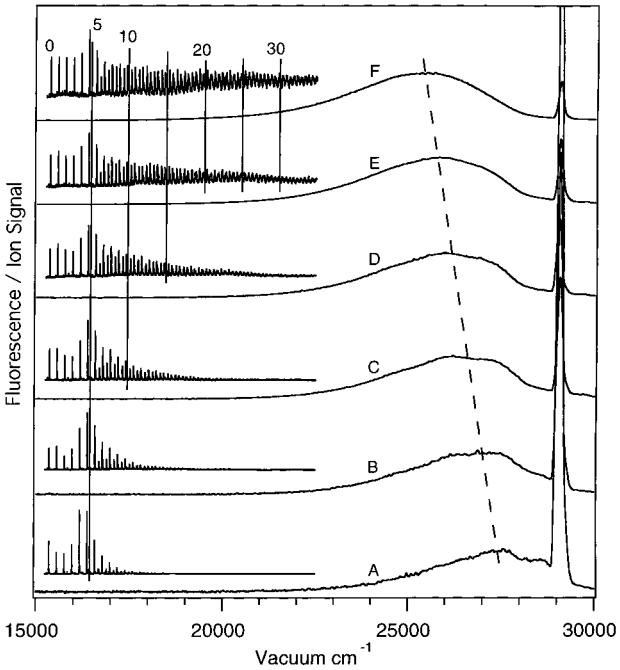

Figure 6. Fluorescence spectra of some 5-cyano-2-naphthol$(CH_3OH)_n$ cluster distributions. The mass spectra corresponding to the fluorescence spectra are inset on the left, and cluster size increments of 5 are indicated with vertical lines. No ESPT emission appears for n up to at least 35. Excitation was at 29100 cm^{-1}, and ionization was at 36350 cm^{-1}. The dashed line indicates the red shift with increasing cluster size. The largest, rightmost peak in each spectrum is predominantly scattered laser excitation light. See text for further discussion.

The second effect observed in fluorescence of larger clusters in Figure 5 may be connected to the "thermally" limited ESPT reaction extent. The bulge and red shift of the molecular fluorescence may be the emission of those clusters that could react at higher internal energy, but are not able to within the lifetime of the excited state at the low temperature of the expansion.

The fluorescence lifetimes of the 5CN2NpOH$(H_2O)_n$ molecular and anion fluorescence bands were found to be different. At 27800 cm^{-1} the lifetime was 22 ± 2 ns, while at 19250 cm^{-1} it was 39 ± 2 ns. Again a delay of 3−4 ns in the temporal position of the long wavelength emission vs the molecular band was observed. These indications are consistent with a model in which the water cluster relaxes after excitation, and this relaxation is necessary for the ESPT reaction. In this respect 5CN2NpOH is remarkably similar in its behavior to 1NpOH in water clusters.

(4) 5-Cyano-2-naphthol Methanol and Me_2SO Clusters. 5CN2NpOH in solution undergoes ESPT to solvents other than water, and the reaction is in every case detected by the strongly red-shifted fluorescence.[2,9] However, except in water, the pK_a* is >0. In methanol it is 2.6, and in Me_2SO it is 0.9.[9] In methanol/water mixtures, small water mole fractions facilitate the reaction considerably, but the pK_a* only drops below zero for compositions of more than 85% water.[4]

These facts and the experience with water clusters above suggest that ESPT in 5CN2NpOH$(MeOH)_n$ clusters might be weak or absent. This is borne out by the results shown in Figure 6.

Despite the relative ease with which large methanol clusters could be generated and detected, no ESPT emission was observed. The fluorescence lifetimes across the spectrum were 30 ns, providing no hint of a weak ESPT band buried under the molecular fluorescence. Residual water in the sample led to mixed clusters containing some water, starting at about n = 6. This also did not enhance ESPT. The position of the molecular fluorescence does shift to the red, as indicated by the dashed line in the figure, but does not change shape as for water clusters. The red shift with increasing cluster size is interesting because of the correlation found in bulk solvents of shift with the Kamlet−Taft beta factor,[2,9] describing the solvent's ability to make a proton-accepting hydrogen bond with the solute. In methanol clusters it seems unlikely that cooperative effects are so extensive that the strength of this hydrogen bond to the OH group is still increasing at n = 30. Rather, increasing extension of the solvent cluster over the ring system is considered a more probable cause for this observation.

TABLE 3: S_1 Electronic Origin Positions and Some Vibrational Frequencies Observed in the R2PI Spectra of the Two Rotamers of 2-Naphthol(NH_3) and 5-Cyano-2-naphthol(NH_3), in cm^{-1} [a]

trans 2N	trans 5C2N	cis 2N	cis 5C2N
29964 (origin)	28886 (origin)	30310 (origin)	29251 (origin)
		34	27
		57	59
			82
		110	
171	166	176	170
	182		
		230	242
	293	283	313
332	348		
	353		
	360	366	
417		417	398
468		458	476
507		507	

[a] The 2-naphthol(NH_3) frequencies are from ref 38, and the 2-naphthol(NH_3) trans/cis assignments are according to ref 54.

The relatively low vapor pressure of Me_2SO limits generation of large clusters in the current apparatus. As a result, only a very narrow distribution could be obtained, consisting of mostly n = 1 and a small amount of n = 2. The fluorescence spectra gave no indication of ESPT. The emission was similar to that of n < 5 water clusters.

Although the size distribution was very limited, this result is interesting because 5CN2NpOH ESPT is strong in bulk Me_2SO.[9,13] Me_2SO being nonprotic, its solvation effect is largely through its good ability to accept hydrogen bonds. This specific feature is believed to be a significant aspect of the ESPT reaction of 5CN2NpOH.[2,9] As a result, Me_2SO might be thought a particularly likely candidate for a proton acceptor whose properties are such that a single molecule, via a single hydrogen bond, could induce ESPT. This was not found to be the case.

(5) Nature of the ESPT Excited States. Discussion of ESPT in naphthols often involves naphthalene-like descriptions of the first two excited states. The S_1 of naphthalene is often labeled L_b in Platt notation and the S_2 is labeled L_a. The naphthalene L_b is derived from two singly excited electronic configurations: HOMO to LUMO+1, and HOMO-1 to LUMO. The L_a is the HOMO to LUMO excited configuration. These descriptions are largely retained in 1NpOH, and to a slightly lesser extent, 2NpOH.[53] The situation is less clear in the excited anion after donation of the proton to the solvent. The lowest excited state is then often assumed to have substantial L_a character, because the L_a is, prior to reaction, more polar. While this is a good starting point, substituents will modify it, especially in the present case, where two are present.

Multiconfiguration self-consistent field calculations were carried out on the singlet states of 1NpOH, 1NpO^-, 2NpOH,

TABLE 4: The Most Important Configurations Contributing to the CASSCF Excited Singlet States of 5-Cyano-2-naphthol and the 5-Cyano-2-naphtholate Anion[a]

5CN2NpOH S_1 vertical		
coefficient	occupancy	
0.367	2212−100	b
0.336	2221−010	b
0.318	2221−100	a
0.183	2212−001	

5CN2NpO$^-$ S_1 vertical			5CN2NpO$^-$ S_1 adiabatic		
coefficient	occupancy		coefficient	occupancy	
0.431	2122−100		0.507	2122−100	
0.321	2221−100	a	0.219	2221−100	a
0.271	1222−100		0.144	2212−100	b
0.105	2122−001		0.141	2022−200	

5CN2NpO$^-$ S_1 PCM vertical			5CN2NpO$^-$ S_1 PCM adiabatic.		
coefficient	occupancy		coefficient	occupancy	
0.434	2122−100		0.506	2122−100	
0.316	2221−100	a	0.213	2221−100	a
0.276	1222−100		0.146	2212−100	b
0.102	2122−001		0.141	2022−200	

2-NpOH S_1 vertical			2-NpO$^-$ S_1 vertical		
coefficient	occupancy		coefficient	occupancy	
0.511	2221−100	a	0.875	2221−100	a
0.456	2212−100	b	0.181	2221−001	
0.438	2221−010	b	0.142	2220−110	
0.268	2212−010		0.137	2211−200	

1-NpOH S_1 vertical			1-NpO$^-$ S_1 vertical		
coefficient	occupancy		coefficient	occupancy	
0.458	2221−010	b	0.826	2221−100	a
0.347	2212−100	b	0.234	1221−101	
0.202	2122−010		0.178	2221−010	b
0.118	1222−100		0.156	2221−0001	

[a] The active "filled" orbitals are followed by the active "virtual" orbitals. The nominal ground state configuration is 2222−000. The anion was calculated at the neutral ground state geometry (vertical excitation) and relaxed to its optimum geometry (adiabatic excitation). These were then recalculated in simulated water solution, using the polarizable continuum model (PCM, in the Gamess package[51]) configurations resembling those making up the L_a or L_b states of naphthalene are indicated by "a" or "b". The basis used was 4-31G(d,p).

2NpO$^-$, 5CN2NpOH, and 5CN2NpO$^-$ to address this question. The calculations were not state-averaged, so as to avoid "premixing" of states and misleading results. In all cases, neutrals and anions, the four orbitals spanning the HOMO−LUMO gap retained similarity in their nodal structure to the parent naphthalene orbitals. At the same time, and in contrast to naphthalene, they became more localized on one ring or the other, especially in the cyano compounds. To the extent that these orbitals can be approximately mapped onto those of naphthalene, Table 4 then shows that the vertically excited S_1 of neutral 5CN2NpOH is mostly L_b in character, with some L_a also included. The L_a and L_b contribute only $^1/_3$ of the configurations making up the state (sum of the squares of the coefficients). The parent 2NpOH also has a rather mixed vertical S_1, the L_b contributing slightly more than the L_a, but these together comprise two-thirds of the state. The vertical 1NpOH S_1 is more like 5CN2NpOH in that the L_b configurations are dominant, but only one-third of the total.

The vertical 2NpO$^-$ and 1NpO$^-$ S_1 states are largely L_a in nature, as expected from the traditional picture. In contrast, the 5CN2NpOH anion is not well described as either L_a or L_b. There is an L_a component, but the state is dominated by excitations of deeper origin (HOMO-2) that do not contribute in naphthalene. This is even more true for the relaxed ("adiabatic") S_1 than for the vertically excited state. Not only does the main configuration become more dominant upon relaxation, but some L_b character is added into the state again. In addition, the configuration labeled "a" is not so clearly of L_a character as in the unrelaxed S_1. The orbitals more resemble a 2212−010 excitation of the unrelaxed anion. There is some transfer of electron density from both CN and O$^-$ to the rings. Similarly, the anion S_2 state has some L_b character, but also large contributions from other configurations. Remarkably, the anion S_1 state is essentially unchanged in simulated water solution. The major configurations are the same and the coefficients nearly identical.

TABLE 5: Calculated Dipole Moments (Debye) of 5CN2NpOH, 2NpOH, and 1NpOH, as Well as Their Conjugate Anions in Ground and Excited States[a]

	ROH S_0	ROH vertical S_1	RO$^-$ vertical S_1	RO$^-$ adiabatic S_1
5CN2NpOH	3.5	3.6	4.3 (4.7)	3.1 (3.6)
2NpOH	1.7	1.3	2.1	
1NpOH	1.2	2.1	4.8	

[a] The values in parenthesis are for simulated water solution (PCM model). The vertically excited states were calculated at the ground state geometry; adiabatic refers to a fully relaxed excited state.

To speak of an "L_a/L_b inversion" upon deprotonation appears to be an acceptable description for 1NpOH and 2NpOH, although the protonated form is not clearly L_b in the 1-isomer. For 5CN2NpOH, however, this is only a very approximate description of the states involved. This is to be expected as the substituent atomic orbitals become increasingly important in the frontier molecular orbitals. Similar difficulties are expected to apply to other cyano-hydroxyarenes. The L_a/L_b terminology was, for example, used in a recent calculational study of cyano-phenol.[57] Such caution is especially warranted if the calculations are "state averaged", or not for pure S_1 or S_2 states, as was the case for cyano-phenol.

Table 5 shows the calculated dipole moments in the neutrals and anions. The neutral cyano compound is more polar, as expected. In the anion S_1 state, 5CN2NpO$^-$ is more like 1NpO$^-$ than 2NpO$^-$. The 5CN2NpOH ground state dipole was oriented at 67° vs the long axis of the ring system, slightly more toward the short than the long axis. The S_1 dipole angle was nearly unchanged at 69°. The unrelaxed anion S_1 was not much different, at 58°. After relaxation into the optimum geometry, the anion S_1 dipole rotated substantially, to 100°, becoming dominantly short axis polarized. This is accompanied by a shortening of the C−O (0.02 Å), and C−CN (0.04 Å) bonds, and lengthening of the C−N bond (0.01 Å). At the same time 0.02 electron charges are transferred from the oxygen to the nitrogen. This rotation is rather similar to that found for 1NpOH, where the much more polar anion S_1 is 43° more short axis polarized than the long-axis polarized neutral. 2NpOH is predominantly short axis polarized in both neutral and anion.

The cyano-naphthol S_1 states are calculated to be about as polar as the ground state. This is initially surprising since the solution fluorescence data show considerable S_1 solvatochromism. The dipole moments are not necessarily a good indicator of polarity in this case, since the polar groups are arranged roughly on opposite ends of the molecule. For example, the cyano group becomes locally more polar in the 5CN2NpO$^-$ adiabatic S_1 compared to the vertical S_1, with a change in net charge of −0.07 to −0.45. At the same time the dipole moment

actually decreases because of compensating charge movement elsewhere. The observed solvatochromism is probably more associated with local interactions rather than a global dipole moment. This is consistent with the conclusions of the Kamlet−Taft analysis of the solvatochromism.[2,9,10]

Moderate calculated polarity in the vibrationless neutral S_1 is consistent with the vibronic coupling model for 1-naphthol ESPT in water and water clusters.[46] Without vibrationally induced S_1/S_2 mixing the S_1 is not believed to be polar enough to trigger the solvent reorganization needed for ESPT. The extensive spectroscopic indications of vibronic coupling found above make this model a strong candidate for 5CN2NpOH as well.

These calculations give some indications of why 5CN2NpOH is found to behave more like 1NpOH than 2NpOH in its cluster ESPT reactivity. The neutral S_1 state is less dominantly L_b or L_a in nature than in 2NpOH, and the vertical anion S_1 is more polar. Vibronic S_1/S_2 coupling may also be more significant and necessary.

Conclusions

Both R2PI absorption and fluorescence emission spectra in the molecular beam indicate that the S_1 states of the free 5CN2NpOH molecule and smallest clusters are analogous to those of the parent noncyano compound 2NpOH. This is supported by calculations showing that the S_1 of the neutral 5CN2NpOH molecule has significant L_b character. Vibronic coupling is found to be stronger than in 2NpOH. It may be associated with increased intramolecular charge transfer, and therefore a factor in ESPT activity.

Strong ESPT was observed in 5CN2NpOH ammonia clusters. The threshold size is 3 or 4 ammonia molecules. This is consistent with the thermodynamic model developed for 1NpOH and 2NpOH, despite the lower aqueous pK_a* of 5CN2NpOH. The anion emission is very similar to that observed in bulk solvents like water, and is delayed by 2−3 ns. It is not yet clear whether the reaction is fast and adiabatic or slower and nonadiabatic in nature.

Moderate ESPT activity was observed in 5CN2NpOH water clusters. In accordance with the lower pK_a* the threshold size is near 10, smaller than that of 1NpOH. The reaction is far less extensive than in ammonia clusters. It is also less extensive under stronger cooling conditions, even when larger clusters are thereby created. This, with the 3−4 ns delayed anion emission, suggests that post-excitation water relaxation is a necessary part of the reaction, and that it is nonadiabatic.

No ESPT activity was observed in large methanol or small Me_2SO clusters, in contrast to the corresponding bulk solutions. In bulk, where the pK_a* values are greater than zero, ESPT proceeds by virtue of thermal activation and entropic contributions. In clusters, the effective temperature is often too low for these factors to play a significant role. The methanol and Me_2-SO cluster data are therefore consistent with the bulk solution results. Indeed, comparison of cluster and bulk data makes the enthalpic vs entropic effects directly visible. This, in turn, illuminates differences between 2NpOH and 5CN2NpOH. The greater enthalpic driving force of the cyano photoacid is able to compensate for unfavorable entropic factors, enabling ESPT in solvents in which 2NpOH ESPT is not found.

While the S_1 of the neutral molecule has significant L_b character, the deprotonated anion is not well described as a L_a state in CASSCF calculations. The "L_a/L_b inversion" description that has been useful for discussion of ESPT in the noncyano compounds therefore has only limited applicability to 5CN2NpOH. The calculated characteristics of the 5CN2NpOH excited states are found to have more similarity with 1NpOH than 2NpOH, consistent with experiment.

In summary, 5CN2NpOH appears to be rather analogous to 1NpOH in its ESPT behavior in clusters. The main indication of its somewhat greater photoacidity is that the cluster ESPT threshold sizes are less than for1NpOH. Much of the model developed for 1NpOH and described in the Introduction may apply to 5CN2NpOH. Understanding the similarities and differences will undoubtedly lead to a more detailed molecular picture of reactive solvent−solute reactions and proton transfer in particular.

Acknowledgment. The authors would like to acknowledge support from ETH internal research grant 0-20402-97 to R.K.; and the U.S. National Science Foundation through a grant to L.M.T.

References and Notes

(1) Tolbert, L. M.; Haubrich, J. E. *J. Am. Chem. Soc.* **1994**, *116*, 10593.
(2) Solntsev, K. M.; Huppert, D.; Tolbert, L. M.; Agmon, N. *J. Am. Chem. Soc.* **1998**, *120*, 7981.
(3) Carmeli, I.; Huppert, D.; Tolbert, L. M.; Haubrich, J. E. *Chem. Phys. Lett.* **1996**, *260*, 109.
(4) Solntsev, K. M.; Huppert, D.; Agmon, N.; Tolbert, L. M. *J. Phys. Chem. A.* **2000**, *104*, 4658.
(5) Pines, E.; Tepper, D.; Magnes, B.-Z.; Pines, D.; Barak, T. *Ber. Bunsen-Ges. Phys. Chem.* **1998**, *102*, 504.
(6) Pines, E.; Pines, D.; Barak, T.; Magnes, B.-Z.; Tolbert, L. M.; Haubrich, J. E. *Ber. Bunsen-Ges. Phys. Chem.* **1998**, *102*, 511.
(7) Pines, E.; Magnes, B.-Z.; Lang, M. J.; Fleming, G. R. *Chem. Phys. Lett.* **1997**, *281*, 413.
(8) Cohen, B.; Huppert, D. *J. Phys. Chem. A* **2000**, 2663.
(9) Solntsev, K. M.; Huppert, D.; Agmon, N. *J. Phys. Chem. A* **1999**, *103*, 6984.
(10) Solntsev, K. M.; Huppert, D.; Agmon, N. *J. Phys. Chem. A* **1998**, *102*, 9599.
(11) Agmon, N.; Levine, R. D. *Chem. Phys. Lett.* **1977**, *197*, 52.
(12) Agmon, N.; Levine, R. D. *Isr. J. Chem.* **1980**, *19*, 330.
(13) Gopich, I. V.; Solntsev, K. M.; Agmon, N. *J. Chem. Phys.* **1999**, *110*, 2164.
(14) Förster, T. *Naturwissenschaften* **1949**, *36*, 186.
(15) Weller, A. *Z. Phys. Chem. Neue Folge* **1958**, *17*, 224.
(16) Weller, A. *Z. Elektrochem.* **1950**, *56*, 662.
(17) Pines, E.; Fleming, G. *Chem. Phys.* **1994**, *183*, 393.
(18) Knochenmuss, R.; Leutwyler, S. *J. Chem. Phys.* **1989**, *91*, 1268.
(19) Knochenmuss, R.; Holtom, G.; Ray, D. *Chem. Phys. Lett.* **1993**, *215*, 188.
(20) Knochenmuss, R.; Smith, D. E. *J. Chem. Phys.* **1994**, *101*, 7327.
(21) Knochenmuss, R. *J. Chim. Phys.* **1995**, *92*, 445.
(22) Knochenmuss, R.; Karbach, V.; Wickleder, C.; S.; G.; Leutwyler, S. *J. Phys. Chem. A* **1998**, *102*, 1935.
(23) Lee, J.; Robinson, G. W.; Webb, S. P.; Philips, L. A.; Clark, J. H. *J. Am. Chem. Soc.* **1986**, *108*, 6538.
(24) Tramer, A.; Zaborowska, M. *Acta Phys. Pol.* **1968**, *34*, 821.
(25) Robinson, G. W.; Thistlewaite, P. J.; Lee, J. *J. Phys. Chem.* **1986**, *90*, 4224.
(26) Knochenmuss, R.; Cheshnovsky, O.; Leutwyler, S. *Chem. Phys. Lett.* **1988**, *144*, 317.
(27) Cheshnovsky, O.; Leutwyler, S. *J. Chem. Phys.* **1988**, *88*, 4127.
(28) Knochenmuss, R. *Chem. Phys. Lett.* **1998**, *293*, 191.
(29) Knochenmuss, R. *Chem. Phys. Lett.* **1999**, *305*, 233.
(30) Knochenmuss, R.; Fischer, I.; Lührs, D.; Lin, Q. *Isr. J. Chem.* **1999**, *39*, 221.
(31) Kelley, D. F.; Bernstein, E. R. *Chem. Phys. Lett.* **1999**, *305*, 230.
(32) Hineman, M. F.; Bruker, G. A.; Kelley, D. F.; Bernstein, E. R. *J. Chem. Phys.* **1992**, *97*, 3341.
(33) Kim, S. K.; Breen, J. J.; Willberg, D. M.; Peng, L. W.; Heikal, A.; Syage, J. A.; Zewail, A. H. *J. Phys. Chem.* **1995**, *99*, 7421.
(34) Siebrand, W.; Zgierski, M. Z. *Chem. Phys. Lett.* **2000**, *320*, 153.
(35) Lührs, D.; Knochenmuss, R.; Fischer, I. *Phys. Chem. Chem. Phys.* **2000**, *2*, 4335.
(36) Connel, L. L.; Ohline, S.; Joireman, P. W.; Corcoran, T. C.; Felker, P. M. *J. Chem. Phys.* **1991**, *94*, 4668.
(37) Yoshino, R.; Hashimoto, K.; Omi, T.; Ishiuchi, S.; Fujii, M. *J. Phys. Chem. A* **1998**, *102*, 6227.

(38) Droz, T.; Knochenmuss, R.; Leutwyler, S. *J. Chem. Phys.* **1990**, *93*, 4520.
(39) Solgadi, D.; Jouvet, C.; Tramer, A. *J. Phys. Chem.* **1988**, *92*, 3313.
(40) Jouvet, C.; Dedonder-Lardeux, C.; Richard-Viard, M.; Solgadi, D.; Tramer, A. *J. Phys. Chem.* **1990**, *94*, 5041.
(41) Pino, G. A.; Dedonder-Lardeaux, C.; Grégoire, G.; Jouvet, C.; Martrenchard, S.; Solgadi, D. *J. Chem. Phys.* **1999**, *111*, 10747.
(42) Grégoire, G.; Dedonder-Lardeux, C.; Jouvet, C.; Martrenchard, S.; Peremans, A.; Solgadi, D. *J. Phys. Chem.* **2000**, *104*, 9087.
(43) Pino, G.; Grégoire, G.; Dedonder-Lardeux, C.; Jouvet, C.; Martrenchard, S.; Solgadi, D. *Phys. Chem. Chem. Phys.* **2000**, *2*, 893.
(44) Steadman, J.; Syage, J. A. *J. Chem. Phys.* **1990**, *92*, 4630.
(45) Jacoby, C.; Hering, P.; Schmitt, M.; Roth, W.; Kleinermanns, K. *Chem. Phys.* **1998**, *239*, 23.
(46) Knochenmuss, R.; Muiño, P.; Wickleder, C. *J. Phys. Chem.* **1996**, *100*, 11218.
(47) Humphrey, S. J.; Pratt, D. W. *Chem. Phys. Lett.* **1996**, *257*, 169.
(48) Magnes, B.-Z.; Strashnikova, N. V.; Pines, E. *Isr. J. Chem.* **1999**, *39*, 361.
(49) Matsumoto, Y.; Ebata, T.; Mikami, N. *J. Chem. Phys.* **1998**, *109*, 6303.
(50) Schütz, M.; Bürgi, T.; Leutwyler, S.; Fischer, T. *J. Chem. Phys.* **1993**, *99*, 1469.
(51) Schmidt, M. W.; Baldridge, K. K.; Boatz, J. A.; Elbert, S. T.; Gordon, M. S.; Jensen, J. J.; Koseki, S.; Matsunaga, N.; Nguyen, K. A.; Su, S.; Windus, T. L.; Dupuis, M.; Montgomery, J. A. *J. Comput. Chem.* **1993**, *14*, 1347.
(52) Oikawa, A.; Abe, H.; Mikami, N.; Ito, M. *J. Phys. Chem.* **1984**, *88*, 5180.
(53) Johnson, J. R.; Jordan, K. D.; Plusquellic, D. F.; Pratt, D. W. *J. Chem. Phys.* **1990**, *93*, 2258.
(54) Plusquellic, D. F.; Tan, X.-Q.; Pratt, D. W. *J. Chem. Phys.* **1992**, *96*, 8026.
(55) Knochenmuss, R. *Chem. Phys. Lett.* **1999**, *311*, 439.
(56) Vener, M. V.; Iwata, S. *Chem. Phys. Lett.* **1998**, *292*, 87.
(57) Granucci, G.; Hynes, J. T.; Millié, P.; Tran-Thi, T.-H. *J. Am. Chem. Soc.* **2000**, *122*, 12243.